CrossMark

Integrated system for site-specific earthquake hazard assessment with geotechnical spatial grid information based on GIS

Han-Saem Kim[1] · Choong-Ki Chung[2]

Abstract An integrated earthquake hazard assessment system with geotechnical spatial grid information was developed based on a geographic information system (GIS). The developed system, built, within the frame of GIS, consists of a database (DB) containing all available site information and processed data in the standard formats, and system software that performs various functions to manage and utilize the data in the DB. The system software is divided functionally into an input module, a geostatistical three-dimensional integration module, a real-time earthquake hazard assessment module, and an output or visualization module. A systematic framework for construction of a geotechnical spatial grid was developed to consider local site response characteristics for target areas. According to the framework, three interrelated assessment procedures were incorporated into the DB on a real-time basis: real-time seismic load determination, real-time liquefaction hazard estimation, and real-time structure fragility evaluation. The DB and these sub-modules of the system software were combined and integrated into a single system to provide a familiar and user-friendly working environment with a standard interface. In addition, the integrated system was imbedded into the Korea Integrated Seismic System server to be linked with real-time seismic accelerations, and a simulation of the system was specifically conducted at Incheon Port, Korea, using two actual earthquake events (the 2013 Baengnyeong and 2014 Taean earthquakes) and one virtual earthquake scenario. The simulation results were visualized as a geotechnical earthquake hazard map to verify the computer-aided real-time assessment framework at the times, when the three notable earthquake events occurred at the nearby Incheon Port.

✉ Choong-Ki Chung
geolabs@snu.ac.kr

Han-Saem Kim
adoogen@kigam.re.kr

[1] Earthquake Research Center, Korea Institute of Geoscience and Mineral Resources, 124 Gwahak-ro, Yuseong-gu, Daejeon 305-350, Korea

[2] Department of Civil and Environmental Engineering, Seoul National University, 1 Gwanak-ro, Gwanak-gu, Seoul 151-742, Korea

🐾 Springer

1 Introduction

Recently, some large earthquakes that have caused considerable damage have occurred within states surrounding Korea: the 2008 Sichuan (M 8.0); 2008 Honshu (M 6.9); 2005 Kashmir (M 7.3); and 2011 Tohoku (M 9.0) earthquakes. The Korean Peninsula has also experienced or been affected by several recent earthquakes such as the 2007 Odaesan (M 4.8), 2013 Shinan (M 4.9), 2013 Baengnyeong Island (M 4.9), and 2014 Taean (M 5.2), and these events have raised concerns within society and also at the nationwide scale (Kim 2014). Because the Korean Peninsula is located in the inner part of the Eurasian Plate, earthquakes and earthquake hazards have not been frequently documented in earthquake records in the past decades, as they have in Japan, Taiwan, and other neighboring countries belonging to the circum-Pacific seismic zone.

However, the number of recorded earthquake events continues to increase each year, and recent cases of earthquake hazards make it necessary to conduct seismic studies in Korea, as geotechnical earthquake hazards, such as liquefaction and landslides, are a significant threat to structures in ports and downtown areas built on seismically vulnerable loose and saturated sandy soils (Chung et al. 2014). Therefore, evaluation of the geotechnical hazards induced by earthquakes has been emphasized recently, in Korea (Kim 2014). Accordingly, understanding a region's seismicity (magnitude occurrence), ground motion, and attenuation characteristics via earthquake perceptibility analyses would be useful beyond simply developing earthquake hazard estimates in terms of expected levels of ground motion (Thomas and Paul 2013).

Seismic disaster management and mitigation require the establishment of effective systems (or methodologies) for spatial information and earthquake hazard assessment. Their complexity dictates the use of an integrated seismic damage assessment methodology based on a computer-aided system, such as geographic information system (GIS) tool (Chung et al. 2014). Therefore, real-time assessment considering site-specific geotechnical earthquake hazards using GIS is appropriate for supporting rapid emergency responses in certain target areas (Drabek and Hoetmer 1991; Kim et al. 2012a). GIS technology enables the multiple spatial analysis usually related to earthquake hazard micro-zonation through data dissemination and management through the linking of databases (DBs) on a one-to-one relationship with an end-user defined by a common identification index or code (Marble and Pequet 1983; Korte 1997; Hohl 1998; Mouroux and Le 2006; Pal et al. 2008; Vahidnia et al. 2010).

For site-specific geotechnical earthquake hazard assessment, it is essential to construct a reliable geotechnical DB that considers the spatial uncertainty or errors of geotechnical properties. These are known in statistics as 'outliers' or 'outlying observations' (Grubbs 1969; Barnett and Lewis 1994). To reduce or remove outliers in measurements, appropriate geostatistical methods are necessary. In the case of using boring data, geotechnical information is provided point-by-point as one-dimensional (1D) soil profiles. Therefore, geophysical and boring datasets must be integrated to construct three-dimensional (3D) continuous geotechnical spatial information structures based on geostatistical methods (Koltermann and Gorelick 1996; Kupfersberger and Deutsch 1999; Weissmann et al. 1999).

In this research, an integrated system for site-specific earthquake hazard assessment with geotechnical spatial grid information based on GIS was developed to respond to earthquake events in near real time. The integrated system consists of a DB and systematic modules. The sub-modules execute various functions (input, geostatistical 3D integration, real-time earthquake hazard assessment, and output or visualization) for managing and utilizing information in the DB. Furthermore, a real-time assessment of earthquake-induced geotechnical hazards was conducted for Incheon Port, Korea, based on a computer-based spatial information system to verify the applicability of the developed system (Chung et al. 2014).

2 Preview of seismic hazard assessment and systems

Seismic disaster management and mitigation require the establishment of an effective system (or methodologies) for assessing spatial information and earthquake hazard. Previous geotechnical information systems and earthquake hazard management systems, which are reflected in current research trends, were reviewed with respect to an integrated system for geotechnical earthquake hazard assessment.

The data used in geotechnical engineering practices encompass a variety of sources of information including in situ investigations, laboratory tests, field monitoring, and computer analyses. These huge amounts of data are used by a large variety of professionals with different backgrounds and interests, necessitating the use of computer technology (such as big data technology). In particular, researchers and practitioners in geotechnical engineering have historically had to manage problems related to the storage, manipulation, and analysis of geotechnical data that exist within a spatial time domain (Chun et al. 2005). Substantial improvements in computer hardware and software over the past several decades have made it much easier to assimilate large volumes of spatial data, and recent advances in computer-based GIS make the data ideally suited for accomplishing the needs of geotechnical engineering (Chun et al. 2007a; Kim 2014).

Site-specific earthquake hazard assessment studies play a major role in identifying and mitigating the potential effects of an earthquake (RADIUS 1999; FEMA 2003; Cinicioglu et al. 2005; 2007; Yeh et al. 2006). Observations of areas that have been struck by strong ground motion in the last few decades have provided enough evidence to suggest that site-specific geotechnical profile influences the site response characteristics induced by site effect and significantly amplify certain period bands of ground motion (Borcherdt 1994; Sun et al. 2008). Seismic waves are amplified as they pass through soil deposits according to site-specific response characteristics (Kim et al. 2012a, b; Youd and Perkins 1978). Thus, the identification of soil deposits susceptible to ground motion amplification is an important task for accurate risk assessment and loss estimation in areas prone to earthquakes (Papadimitriou et al. 2008; Gorvindaraju and Bhattacharya 2012). Cinicioglu et al. (2007) convinced that strong ground shaking is considered to be the primary earthquake hazard source, whereas earthquake-induced geotechnical hazard such as liquefaction, seismic-bearing-capacity degradation, and landslides are among the main secondary causes of structural damage.

Several site-specific earthquake and hazard assessment methodologies have been applied worldwide (ATC-13 1985; King and Kiremidjian 1994; Schneider and Schauer 2006). Earthquake hazard assessment methodologies are applied mainly for two purposes: to assess damage in urban areas and to plan land use in undeveloped areas of cities. The

conventional approach has low practical application due to unsystematic process logic, but it can be utilized as sub-function for decision-making process of specific earthquake-induce hazards. If a fully systemized evaluation were to be used, a set of probabilities would be presented for each damage-causing hazard (Crowley et al. 2004; Cinicioglu et al. 2005, 2007; Xu and Liu 2009). Therefore, the development of the GIS-based real-time system of this study was begun with the following aims: data processing to construct well-defined standard data formats, real-time seismic monitoring and hazard assessments, complementary data processing, and geostatistical processing.

3 Concept of real-time framework for earthquake hazard assessment

The integrated framework consists of a DB and systematic modules. The DB contains all of the field data and processed data in the system. The sub-modules execute various functions for managing and utilizing information in the DB: input of data, geostatistical 3D integrated data based on input data, real-time earthquake hazard data, and output of data. The framework including all of these functions focuses on user-friendliness and real-time applications. Figure 1 details the integrated framework.

The DB is the backbone of the developed framework. It stores not only primarily collected data such as geography, geotechnical data, structural information, and real-time-based transmitted seismic monitoring data from a seismometer server (from the Korea Integrated Seismic System [KISS]) but also secondary processed data obtained from geostatistical 3D integration and real-time earthquake hazard assessments (Chun et al. 2007a, b). It contains these data as alphanumeric values according to standard formats. The data stored in the DB can be easily utilized in the framework. The input function provides an effective way to store and arrange all collected field data, including electric and non-electric documents, and data on geography, geotechnical investigations, structure-related properties, seismic monitoring, and analyses results, according to a standard format based on a geo-DB (GDB) (Chun et al. 2007b).
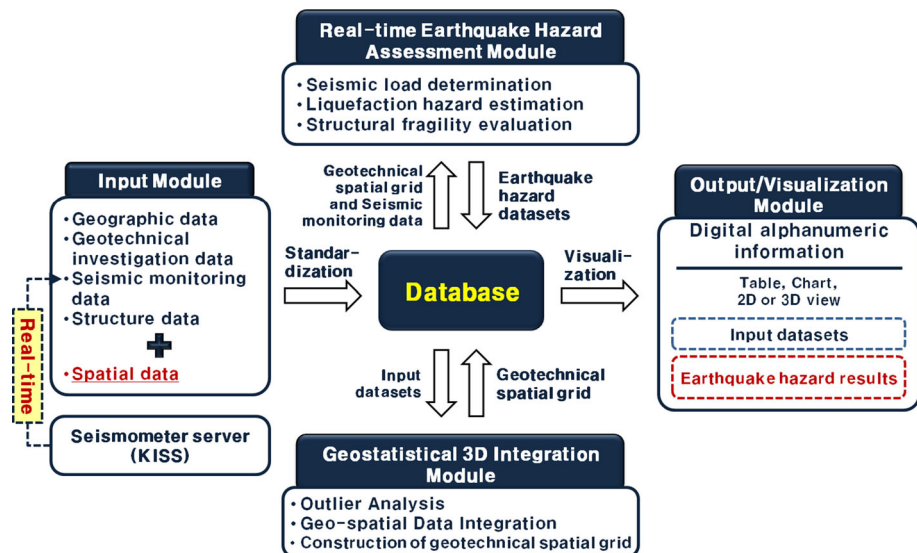

Fig. 1 Integrated framework with geotechnical earthquake hazard assessment procedures

A methodology for near real-time earthquake hazard assessment was proposed using the schematic concept shown in Fig. 2. The arrows represent the sequential data processing. The graphical schematic flow of the integrated earthquake hazard assessment with geotechnical spatial grid information (composed of two systematic functions for geostatistical 3D integration and real-time earthquake hazard assessment) is shown in Fig. 2 (Kim 2014). To determine reliable geotechnical characteristics of a site with seismic risk potential, geostatistical 3D integration using geophysical tomography and borehole soil profile data is established based on a GIS platform. In addition, interrelated procedures for real-time assessment of the earthquake hazard were developed using geotechnical spatial grid information to consider the characteristics of the response of local sites.

The geostatistical 3D integration for the geotechnical spatial grid function constructs distributed 3D geotechnical data over a selected domain from input data acquired from the target site by applying geostatistical methods. This method has three functional modules with the DB: outlier detection, geostatistical integration, and construction of a geotechnical spatial grid. The geotechnical investigation results always reflect the level of soil uncertainty. To determine the uncertainty, two outlier detection methods (a method based on cross-validation and one based on the generalized extreme value distribution) proposed by Kim et al. (2012a, b), which optimize the borehole datasets, are used. In addition, the geostatistical integration method based on indicator kriging is performed using optimized borehole and digitized geophysical tomography data to construct a 3D geo-layer (Kim 2014). The 3D geo-layer is categorized and subdivided into representative soil profile and dynamic properties to assign a 3D geotechnical spatial grid into the DB. This step must be conducted as a baseline prior to the occurrence of earthquakes (Kim 2014).

The real-time earthquake hazard assessment function has three functional modules with the DB: real-time seismic load determination, real-time liquefaction hazard estimation, and real-time structure fragility evaluation. In the first phase, which is linked with the 3D geotechnical spatial grid, correlations between rock outcrop acceleration and maximum acceleration of each layer considering site response characteristics are predetermined (Kim et al. 2002; Kim 2014). Thus, as earthquake events occur and as soon as monitored rock
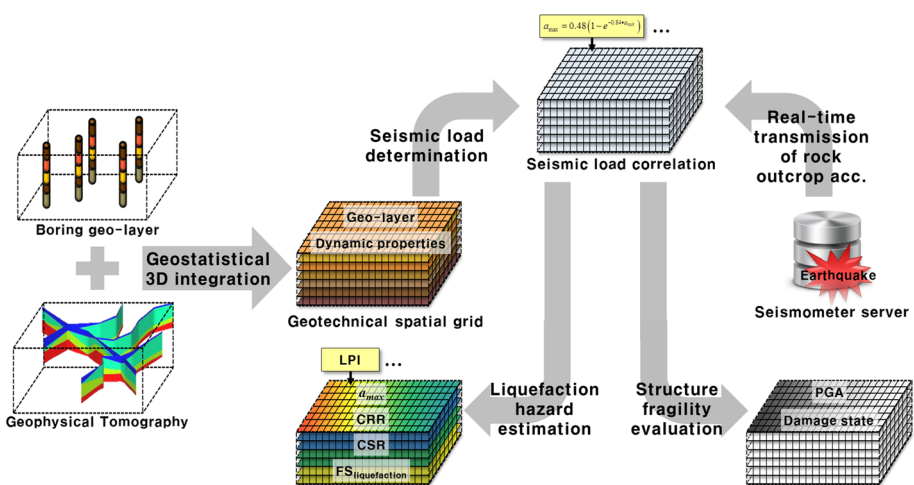

Fig. 2 Schematic flowchart of integrated earthquake hazard assessment with geotechnical spatial grid information

outcrop acceleration data are transmitted from the accelerometer, the seismic load at each spatial grid is estimated. In the second phase, the potential damage due to liquefaction is estimated by integration of the geotechnical spatial grid and correlated maximum acceleration of each layer based on the simplified liquefaction evaluation method (composed of the cyclic stress ratio and the cyclic resistance ratio) using the liquefaction potential index (LPI) in real time (Chung et al. 2014). As earthquake events occur, the LPI and liquefaction severity class are estimated based on correlations with the maximum acceleration of each layer in real time. In the third phase, the structure failure is evaluated in real time by integrating the geotechnical spatial grid and the correlated maximum acceleration based on the structure fragility curve, which is the function that represents the excess probability of the defined damage level for specific earthquake intensity. The correlated peak ground acceleration (PGA) is used as an intensity index of the fragility functions, and the probabilities of failure are calculated. Subsequently, damage grades of superstructures, which depend on the probabilities of failure, are determined. The integrated earthquake hazard of the target structure is determined as a zonation map considering liquefaction and fragility grade (Kim 2014).

The output function displays all attributive information in the DB using tables and graphics according to its characteristics, either on screen or as a document. In addition, all data in the DB can be outputted as a chart or a graphic (Chun et al. 2007b). The graphic functions, such as 2D plane view, 2D sectional view, and 3D view, display interpolated data with field data over an arbitrary domain at the same time. Then all of the charts, graphs, and drawings can be printed. In particular, the earthquake hazard can be visualized and forecasted as 2D or 3D maps overlain by satellite images, and the seismic severity (composed of seismic load, liquefaction, and structure fragility) of the target structure can be determined in real time using zonation criteria.
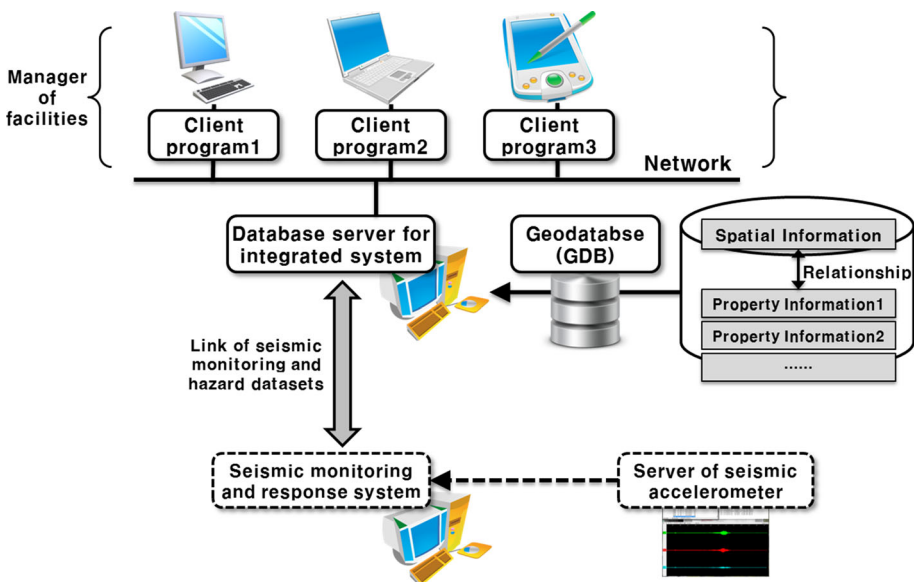

Fig. 3 Operating schema of the developed system

Several assumption conditions and preceding assessments are used to estimate the possible geotechnical earthquake hazard for a target site in real time, as soon as the earthquake occurs. The procedures for considering the site-specific seismic response of the overall target area prior to the occurrence of an earthquake consist of the building of the DB, construction of the geotechnical spatial grid, and site response analysis. As an earthquake occurs near a target site, the possible hazard can be estimated in real time by linking with the rock outcrop acceleration data monitored by accelerometer.

4 Integrated system for real-time earthquake hazard

4.1 Composition of the system

The developed system is hosted on a secure intranet or local area network, and it follows the client–server model in which multiple client PCs request data from a single server with a GDB (Chun et al. 2007b). System software services the client's information needs. The operating schema of the developed system is shown in Fig. 3. From the seismic monitoring and response system of the KISS, the seismic monitoring datasets that are transmitted from the seismic accelerometer server are linked to the DB server for an integrated system, and the earthquake hazard datasets analyzed from the developed system are forecast in real time by the response system.

A system structure consisting of a GDB and four sub-modules was established, as shown in Fig. 2 (Chun et al. 2007b). As the client program, an input module provides an efficient method to store and arrange all obtained field data in the GDB according to standardization of data. In the geostatistical 3D integration module, reliable 3D continuous geotechnical information is determined and the geotechnical spatial grid is constructed into the DB. In the real-time earthquake hazard assessment module, the geo-spatial earthquake hazard is estimated in real time by linking with measured rock outcrop accelerations. The output and visualization module provides functions such as graphs, 2D plane views, 2D sectional views, and 3D views, together with tabular formats (Chun et al. 2007a, b). Moreover, the earthquake hazard can be visualized in real time with the 2D or 3D digital map. With the system software installed on a client PC running the GIS software, connected to the server by a real-time-based network, a user manages and utilizes the information in the GDB. Field data or predetermined estimated hazard results can be entered very simply into the GDB. Once built, all datasets can easily be utilized in each sub-module of the client program (Chun et al. 2007a).

4.2 The DB

The core component of a GIS-based system is the GDB having spatial domain information, which must be obtained and accessible. The main advantage of a GDB is that it allows GIS to build based on the relational DB management systems (RDBMSs). GDB includes the support of the structured query language and the function to generate complex geo-spatial queries (Chun et al. 2007b). In addition, a GDB's client–server architecture enables to simultaneously multi-access, edit, view, and query the GDB considering spatial correlations among input datasets (Chun et al. 2007a, b). To build the optimized GDBMS of the system, a Microsoft SQL server was chosen because of the robustness and scalability of its GDBMS (Chun et al. 2007b). The GDB contains information on all six classes: four
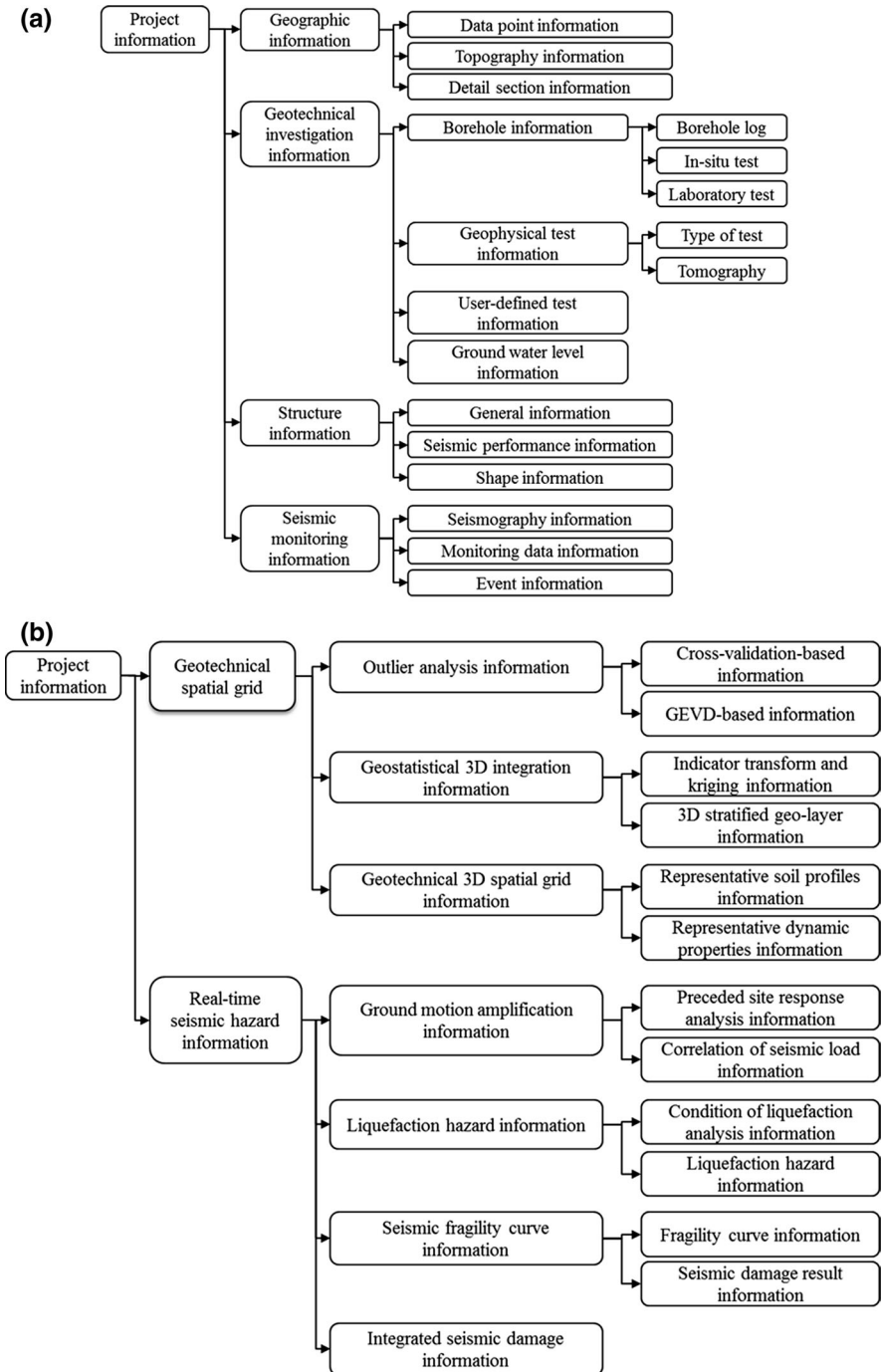
Fig. 4 Key data classes and relations of the GDB for the developed system: **a** primary information; **b** processed information

primarily collected field information and two processed data. The data were standardized by establishing a relationship between geographic coordinate information and other attribute information (Fig. 3). The primary classes of the data model and relations between these classes are shown in Fig. 4 (Chun et al. 2007b; Kim et al. 2010).

GDB is the basic data format for GISs to refer to attribute information and to correlate and analyze various datasets spatially (ESRI 2006). The GDB of the developed system was established based on a 3D coordinate system. Sub-areas of a wide target area are generally used in fields to promote the efficiency of site-specific earthquake hazard management. In addition, a digital map can be used as basic topographic information of the system because it offers an easy way to construct topographic information for a target area. Detailed descriptions of tables for project information in the developed system are shown in Tables 1, 2, 3, 4, 5. The project information is the uppermost category in the hierarchal DB system.

Geotechnical investigations were performed to identify the field ground conditions and to evaluate the engineering parameters of the ground. The quality and quantity of geotechnical investigations depend on the importance and reliability of the current site conditions, but generally, types of geotechnical investigation are categorized into boring inspections, in situ tests, laboratory tests, and geophysical tests. The boring log, which is the basis of geotechnical investigation data, must be utilized in the GDB. Generally, in most ports or urban areas in Korea, the cone penetration test (CPT) and the field vane test (FVT) are frequently performed. Therefore, CPT and FVT data need to be predefined. Engineering parameters evaluated from in situ tests and laboratory tests are also important. Particularly, dynamic tests, such as the shear wave velocity test, the cyclic triaxial test, and the resonance column test, are standardized for the consideration of the dynamic properties of the target site (Sun et al. 2015). Geophysical tests, which consist of seismic refraction

Table 1 Tables for geotechnical investigation information in the developed system

Category	Sub-category	Comment
Borehole data	General description of boring	Boring data, inspector, address, etc.
	Geo-layer data	Description of each geo-layer
	SPT data	Standard penetration test value (SPT-N) with depth
	RQD/TCR data	RQD and TCR with depth
In situ test data	CPT data	Summarized and raw data for CPT and CPTu data
	FVT data	Summarized and raw data for FVT data
Dynamic test data	Shear wave velocity test data	Summarized and raw data for shear wave velocity test data
	Resonance column test data	Summarized and raw data for resonance column test data
	Cyclic triaxial test data	Summarized and raw data for cyclic triaxial test data
Soil material properties	–	Engineering parameters evaluated from various tests
User-defined data	–	Raw data for laboratory tests and undefined in situ tests
Geophysical test data	–	Summarized and raw data for geophysical test data
Groundwater level data	–	The highest daily average GWL from annual GWL record

Table 2 Tables for structure information in the developed system

Category	Comment
Structure information data	Structure type, shape, repair status, structure report, etc.
Structure shape	Spatial coordinate, geometry, etc.

Table 3 Tables for seismic monitoring information in the developed system

Category	Comment
Seismological observatory data	Station name, type, coordinate, etc.
Seismic monitoring data	Summarized and raw data for seismic monitoring data
Earthquake event data	Summarized and raw data for earthquake event

tests and resistivity tests, are essential for retaining rational continuous geotechnical properties. Raw test data from in situ tests, laboratory tests, and earthwork results (design or construction reports) are also necessary on occasion. Therefore, geotechnical investigation information consists of borehole log data, in situ test data, dynamic test data, engineering parameters evaluated from various tests, user-defined data, and geophysical test data, and geotechnical investigation data are standardized. According to the results from the standardization, the brief DB structure for storing geotechnical investigation information can be shown as demonstrated in Table 1.

From the in situ tests, classification criteria of liquefiable geo-layers and non-liquefiable geo-layers can be determined. A geo-layer with liquefaction potential is defined as porous geo-material below the groundwater level (GWL). To estimate the reliable GWL data considering fluctuations such as the effects of rainfall, drainage system, or tides at coastal areas, the highest GWL was selected for conservative estimation of seismic load and liquefaction hazard. The highest daily average GWL during the monitoring period from the annual GWL record at the target site is utilized and additionally composed as primary information of the DB (Chung et al. 2014). And the liquefiable geo-layers are selected based on the basic conditions of the liquefaction hazard estimation and applied to the procedure.

Structure information can be considered to reflect the seismic performance capacity, and it can be obtained from a building register and performance appraisal report. A brief DB structure for storing structure information is shown in Table 2. Prior to forming an explanation for the data structure of the seismic monitoring information, it is necessary to look into the operating mechanism of the instruments, types of instruments, and so on. As the seismic accelerations are transmitted in real time from the KISS, the data format for an earthquake event according to KISS is designed to consider the event trigger time and transferred event file. The data format for an earthquake event (belonging to the KISS server) was previously arranged for the target area, Korea. For seismic monitoring on a real-time basis, seismological observatory data, seismic monitoring data, and earthquake event data are standardized as shown in Table 3.

The geotechnical spatial grid information in the system consists of the results and the options of the geostatistical 3D integration procedure (Table 4). The results are a grid model over a selected domain, and the options include information related to the geostatistical method and the gridding of the selected domain, which are excluded outliers of borehole datasets. The real-time earthquake hazard information consists of earthquake

Table 4 Tables for geotechnical spatial grid information in the developed system

Category	Comment
Indicator kriging data	Kriging type, variogram model, etc.
3D geo-layer data	Summarized and raw data for geostatistical integrated layer data
Geotechnical spatial grid data	Summarized and raw data for geotechnical spatial grid data

Table 5 Tables for real-time earthquake hazard information in the developed system

Category	Sub-category	Comment
Seismic load data	Correlation equation data	Correlation coefficient for correlation equation of seismic load
	ProShake results data	Summarized and raw data for ProShake output
	Correlated PGA data	Correlated PGA results
	Correlated PGA of layer data	Correlated PGA of layer results
Liquefaction hazard data	CRR data	Summarized and raw data for cyclic resistance ratio data
	CSR data	Summarized and raw data for cyclic stress ratio data
	FS data	Summarized and raw data for factor of safety for liquefaction data
	LPI data	LPI and liquefaction severity class data
Structure fragility data	Fragility grade data	Structure fragility curve and damage level data
	Fragility damage data	Fragility damage class data
Integrated seismic damage data		Integrated seismic damage associated with liquefaction and fragility class data

hazard assessment results and analysis options. The earthquake hazard results contain the seismic load correlation determination results, liquefaction estimation results, and structure fragility evaluation results (Table 5), and the hazard information is determined automatically and stored in the DB with geotechnical spatial grid information.

4.3 System program

The management of the input or analysis results data is the fundamental and indispensable function for running the system software based on the GDB. All of the collected field data are stored along with their locations in the GDB based on the established standard formats. Therefore, prior to the input of the attribute information, the earthquake hazard information must be inputted into the GDB. These data are managed in an independent window according to the DB structure. Based on the management module, sub-modules are combined with an automated linking procedure: input, geostatistical 3D integration, real-time earthquake hazard assessment, and 3D visualization modules. The sequential systematic procedures for earthquake hazard assessment are programmed by integrating the sub-modules (Fig. 5).

The main management program has various functions: menu, map view, layer content, visualization tool, and site information. From the menu, when users select the menu function, the related sub-modules can be implemented as sharing DBs. Site information inputted from the input modules and the geotechnical spatial grid, and the earthquake hazards estimated real-time framework, are visualized in the map view, which displays a
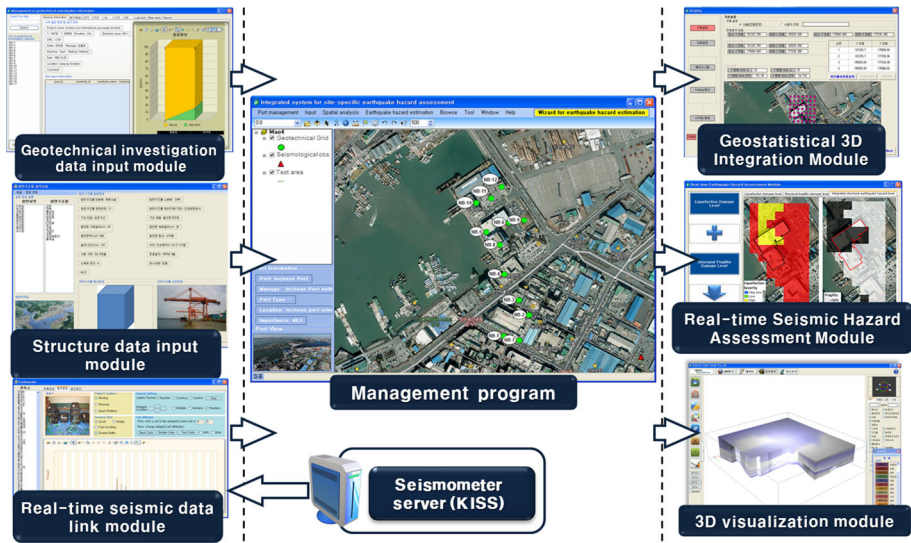
Fig. 5 Systematic procedure of real-time earthquake hazard assessment according to the system program

2D or 3D spatial distribution of the satellite map. Project and topographic information of the target site are managed in the same window because this information is generally used to identify locations of attribute information spatially. In addition, digital or satellite maps of the target area are directly converted into the topographic information of the digital elevation model (DEM) based on previously performed GIS works. Elevation layers of the digital map are spatially interpolated into the DEM information, and geographic features (e.g., roads, buildings, water systems) or a satellite image can be digitized on the over-lapped DEM (with the same coordinate system) using commercial GIS software. Considering the efficiency of the data management, input of geographic information for sub-area information and attribute information was designed to be performed in input windows for attribute information. The geographic information for the attribute information is used to display the locations of the attribute information on a topographic map, that is, a background map, and to utilize the attribute information in the geostatistical 3D integration procedure. The windows for managing the geographic information for the target site are shown in Fig. 6a.

All geotechnical investigation information is managed in a window according to sub-classes. The management modules for borehole information and geophysical testing information are shown in Fig. 6b. General descriptions for boreholes including geographic location and geo-layer information are managed, and geophysical tomography data are digitized using the digitizing tool of the management module. These windows for managing the geotechnical investigation information are designed according to the DB structures and the characteristics of the geotechnical investigation information.

Structure information is stored in the DB of the integrated system (Fig. 6c). The standard structure data inputted using text and image classes, the structure fragility function, and the design report are automatically transformed in the DB. All seismic monitoring information is managed in a window according to sub-class, the same as other input modules. Figure 6d shows management screens of seismic monitoring information
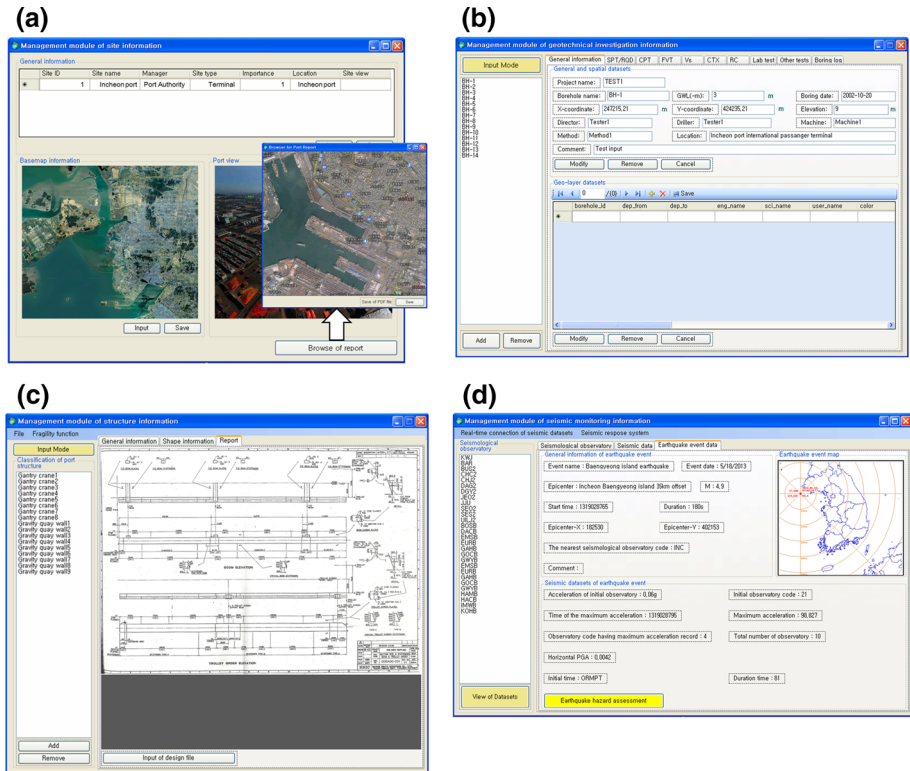
Fig. 6 Management module for input datasets: **a** management module of site information; **b** management module of geotechnical investigation information; **c** management module of structure information; **d** management module of seismic monitoring information

according to sub-class. The geographic location and types of seismometers for a filed monitoring point are defined. The seismic monitoring datasets transmitted from KISS are linked in real time with the nearest accelerometer located at the target site, and the earthquake event information is confirmed as acceleration-time series data and PGA data.

The geostatistical 3D integration module performs the outlier analysis and geostatistical interpolation to produce an evenly spaced grid of values or a selected domain form of the known datasets. Because the integration procedure is somewhat complex, it is necessary for users to have some knowledge of kriging and variograms. Thus, the geostatistical 3D integration module is constructed in a wizard form without knowledge of statistical methods. It is also possible to execute the integration procedure in detail.

The integration module can be applied to all attribute information related to the corresponding geographic information in the GDB, which are geo-layer data, 3D geotechnical spatial grid, and earthquake hazard assessment results with transmitted seismic monitoring data in real time, as earthquake events occur. Figure 7 is an integration screen according to the order of the integration procedure. The wizard functions for sequential geostatistical integration are arranged (Clayton and Andre 1997; Lee and Wong 2001). Selection of a domain and gridding of a selected domain for integration are performed, and attribute data for integration are selected. Then the indicator kriging procedure is performed. After that,
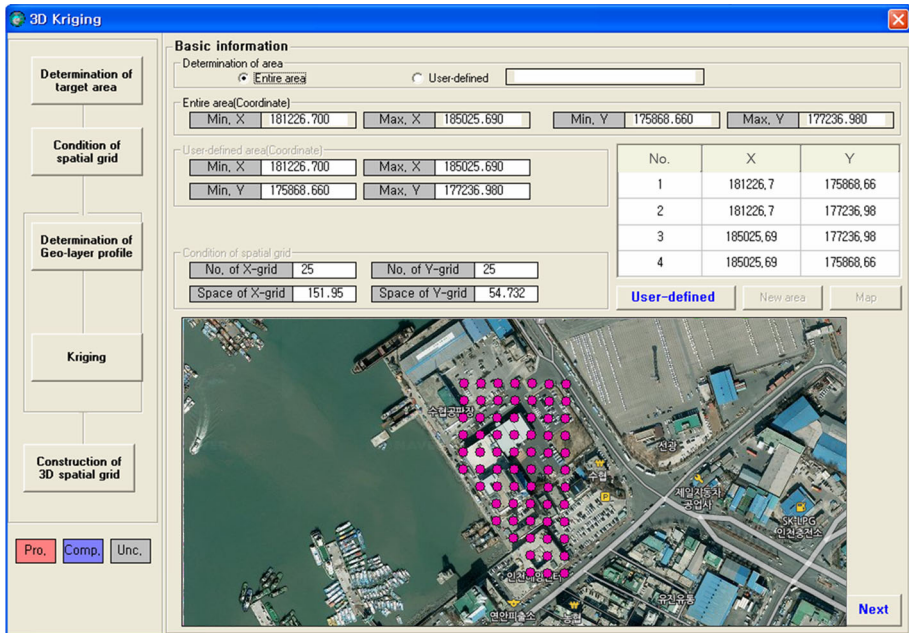
Fig. 7 Geostatistical 3D integration module

the 3D geotechnical spatial grids are determined with the selected domain and linked to the DB for the real-time earthquake hazard assessment module.

Although earthquake events and hazards occur rapidly over a wide region, site-specific earthquake hazard assessment is established by considering the reliable seismic load, severity of liquefaction, and structure fragility based on a geotechnical spatial grid. In addition, these methods are not simply applied for various conditions but rather provide possible earthquake hazards in every instance. Therefore, the wizard functions for sequential real-time earthquake hazard assessment are developed in the integrated system, as shown in Fig. 8. If earthquake events are detected and seismic monitoring data can be transformed in real time, the determination of seismic load, estimation of liquefaction hazard, and evaluation of structure fragility are automatically forecast in real time. The wizard functions for these three procedures are arranged on the left side of the windows.

Users desire to confirm the user-defined information in the GDB to be aware rapidly of emergency hazard condition. The output of the attribute information, which is provided by graphic user interface (GUI), can be displayed in tabular form and graphic form. Table is typically used for input, editing, and view of information in the GDB, and graphical objects provide intuitive views of the spatial relationship between attributive information. The output module displays all attribute information in the GDB using tables and graphic objects in accordance with its characteristics and GDB schema. The 3D integration results are displayed in 2D and 3D images on a computer screen with field information over a selected domain (Chun et al. 2007a, b; Kim et al. 2010). The 3D visualization module is an independent program that was developed considering its application in other GISs. This module was designed based on a large amount of background research on previous commercial GIS software, such as ArcGIS, GDM, Suffer, EVS, Eardas Imagine. The
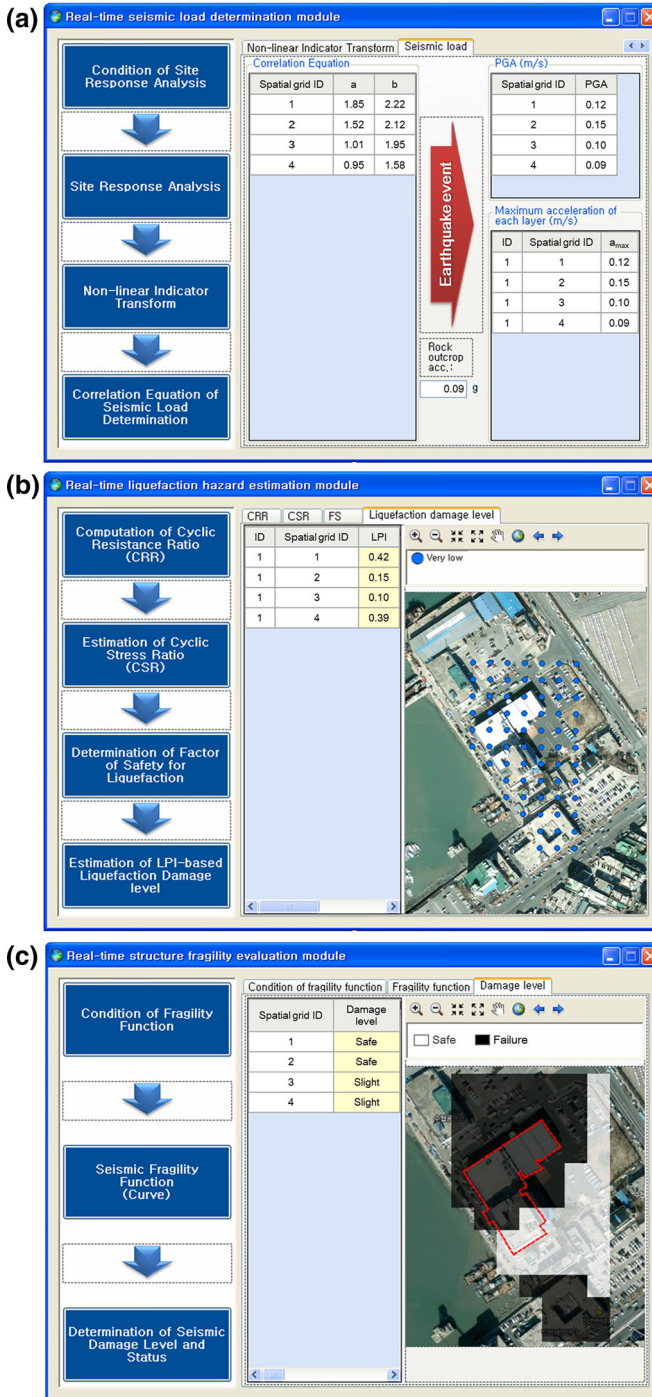
Fig. 8 Three-phase real-time earthquake hazard modules: **a** real-time seismic load determination module; **b** real-time liquefaction hazard estimation module; **c** real-time structure fragility evaluation module

module was programmed by a professional programmer based on our design. The 3D visualization module is executed on a 3D spatial coordinate system for selecting integrated data, as shown in Fig. 9, and these views are representative screens of the geotechnical spatial grids and real-time basis earthquake hazard results.

5 Systematic field application for Incheon Port in Korea

5.1 Simulation conditions

The integrated system was installed in the seismic monitoring and response system server and embedded at KISS to manage the seismic risk of a major port area in Korea, and constant monitoring of earthquake events has been conducted since 2010 (Chung et al. 2014). In 2013 and 2014, noticeable earthquake events occurred in the waters west of Baengnyeong Island and Taean, and seismic monitoring datasets were measured from the accelerometers installed at the coast pier of Incheon Port. Two accelerometers are installed at the testing site to monitor free-field ground motion (at the lock) and structure motion (at the passenger terminal) (Fig. 10).

Therefore, in this research, to verify the integrated system, the actual earthquake events and monitoring dataset were applied preferentially. The testing site is a partial area of the coast pier of Incheon, and 12 borehole datasets were stored in the system DB. The distance from the accelerometer to the extended target area was 0.7 km, and the attenuation effect was negligible. Figure 10 describes the verification test conditions for the earthquake scenarios with the real-time transmission of the seismic monitoring data for each earthquake event.

The conditions of the monitored earthquake events for the verification tests were obtained from the Korea Meteorological Administration (Table 6; Fig. 11). The magnitude
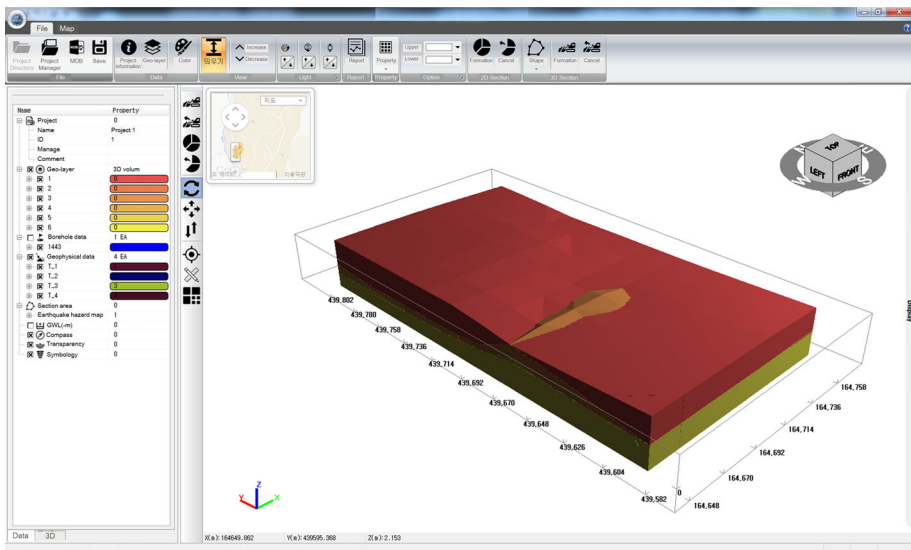
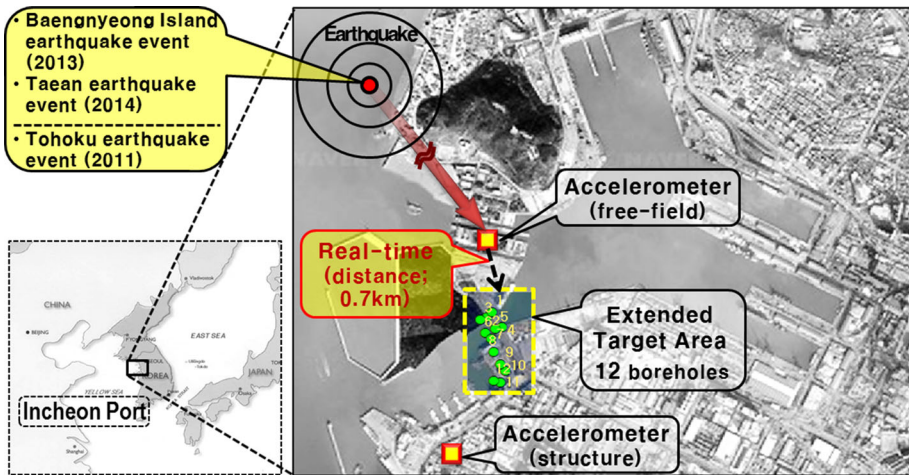

Fig. 9 Three-dimensional visualization module

Fig. 10 Systematic field application conditions for earthquake scenarios for Incheon Port, Korea

of the Baengnyeong Island earthquake event was 4.9, and the epicenter was located in waters west of Incheon Port (distance of about 41 km). The magnitude of the Taean earthquake event was 5.1, and its epicenter was also located in the waters west of Incheon Port (distance of about 141 km). The Taean and Baengnyeong earthquakes were the fourth and fifth largest magnitude earthquakes, respectively, since seismic monitoring began in Korea (1978).

Unfortunately, because strong earthquake events have not been recorded to the present, a hypothetical earthquake for the comparative verification tests had to be simulated to consider the earthquake hazards under the strong-motion condition. For the application example, the 2011 Tohoku earthquake (magnitude 9.0), with the monitoring record 150 km from the epicenter, was applied. The input rock outcrop acceleration was determined to be 0.37 g through the ground motion attenuation relation (Campbell and Bozorgnia 2003) considering the comprehensive trend of ground shaking in Korea.

5.2 Geotechnical spatial grid

The geotechnical spatial grid was determined taking into account the site-specific site conditions of the target port with regard to the computerized geotechnical spatial grid

Table 6 Information on earthquake events and measured results

	Baengnyeong Island earthquake event	Taean earthquake event
Magnitude	4.9	5.2
Date and Time (KST)	2013.05.18, 07:02:24	2014.04.01, 04:48:35
Location (lat, lon)	37.68, 124.63	36.95, 124.58
arock (g) at free-field accelerometer	0.0032	0.0065
Acceleration (g) at structure accelerometer	0.0249	0.0441

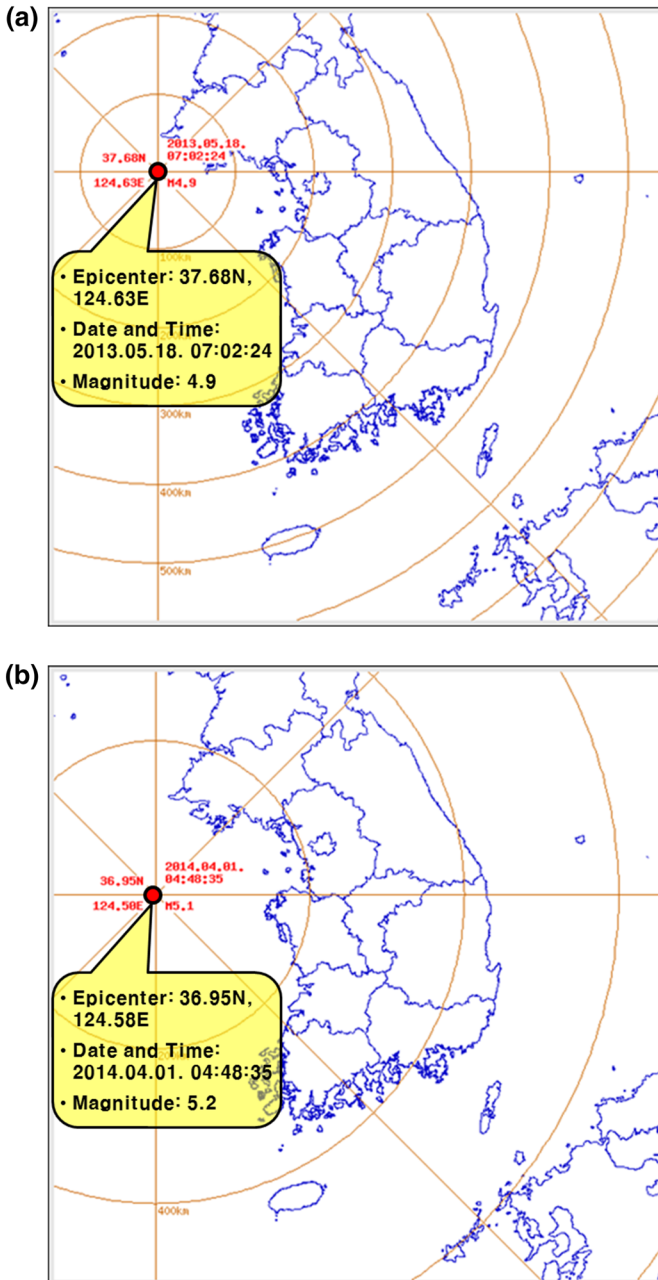*Source*: Korea Meteorological Administration

Fig. 11 Earthquake event map (source: Korea Meteorological Administration): **a** Baengnyeong Island earthquake event; **b** Taean earthquake event

construction procedure using the geostatistical 3D integration module, as shown in Fig. 12. These observation sites were referenced by spatial coordinates determined by GPS (Sun 2004; Sun et al. 2008; Chung et al. 2014). Because interpolation was expected to produce more reliable spatial predictions than extrapolation (Sun et al. 2009), geotechnical spatial grid construction was applied to the extended area (73,600 m^2) including the study area (19,200 m^2). Therefore, 68 cells of the geotechnical spatial grid (covering the ground surface) with constant 20 m intervals were selected for the study area (Chung et al. 2014).

Based on the geotechnical spatial grid, the site-specific earthquake hazards were visualized on a location map (Kim et al. 2012a, b) to confirm the applicability of the real-time estimation of the seismic load, liquefaction, and structure fragility based on the developed management program. To verify the spatial variation in the ground conditions causing earthquake hazards of the study area, we analyzed the variation in depth to bedrock based on the geotechnical spatial grid (Fig. 13). The depth to bedrock is a specifically important geotechnical parameter when evaluating seismic ground amplification and the corresponding structure seismic fragility (Toprak and Holzer 2003; Sun et al. 2008). Concerning the geotechnical spatial grid of the depth to bedrock defined as the soft rock or total soil
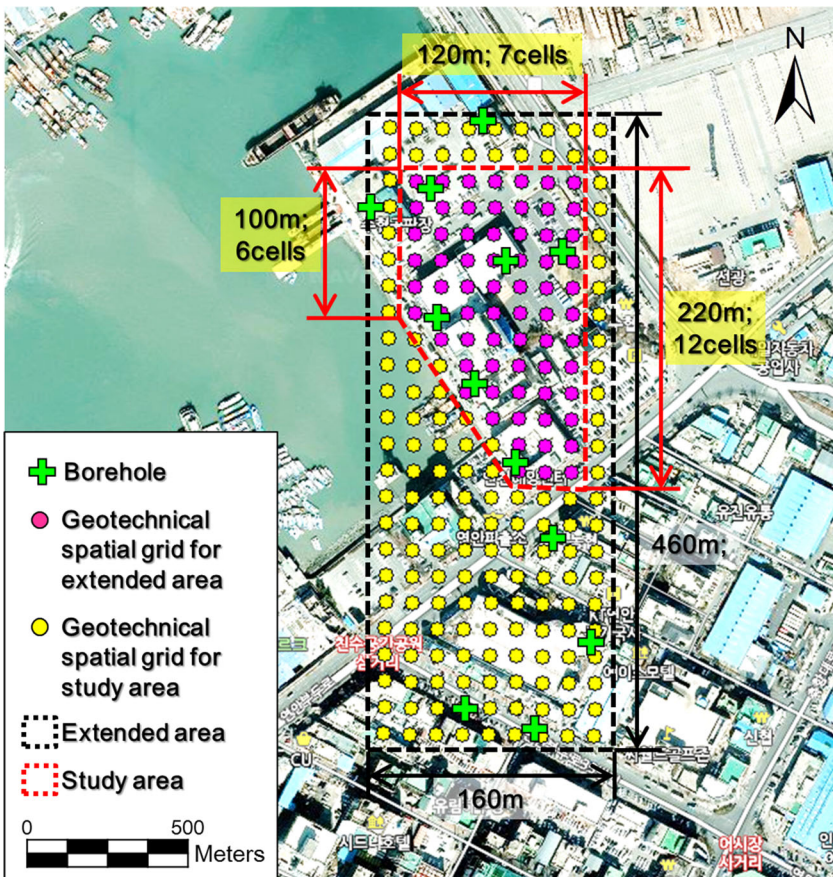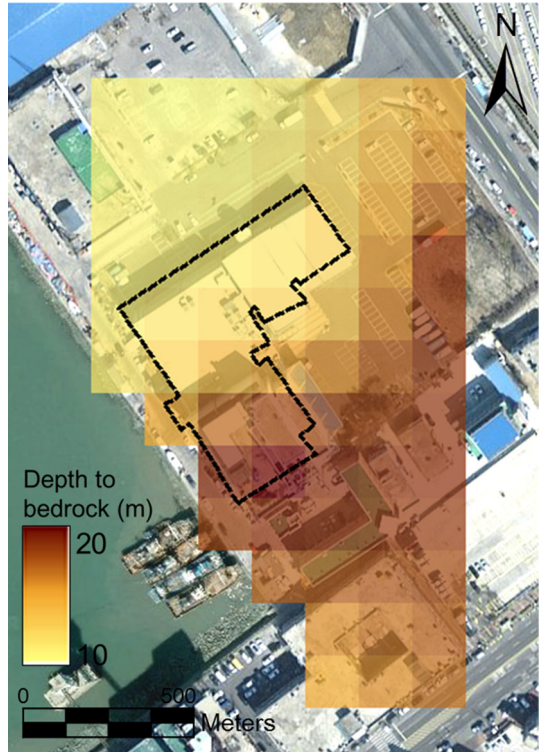

Fig. 12 Condition of geotechnical spatial grid for the target port

Fig. 13 Two-dimensional spatial distribution of the depth to bedrock based on the geotechnical spatial grid for the study area of Incheon Port

profile thickness, the depth to bedrock was greater (about 20 m) toward the south of the target building.

The thicknesses of the geotechnical layers and the depths to bedrock are usually visualized as volumetric grid on the corresponding 3D contour maps to provide more realistic ground conditions using the 3D visualization module (Fig. 14) (Chung et al. 2014). The 3D spatial distribution of the soil profile assigned with dynamic properties by soil type was categorized (Wair et al. 2012) according to the American Society for Testing and Materials (1985), and bedrock (such as soft rock, normal rock, and hard rock) was classified in accordance with the International Society for Rock Mechanics (1981). The soil layers used for fill soil were classified mainly into well-graded gravel–sand mixtures (GW) or silty sand (SM), as shown in Fig. 14a. Figure 14b shows the 3D spatial distribution of the shear wave velocity (V_S), which are ranged from about 400 to 700 m/s for soil deposit, derived from the SPT–N values using empirical correlation between SPT-N and V_S (Sun 2004).

5.3 Integrated earthquake hazard

The geotechnical spatial grids (with 68 cells over the surface) were constructed in advance using 12 borehole datasets based on the geostatistical 3D integration module. Linked with geotechnical spatial grid, the correlations between the rock acceleration and PGA were determined for every 68 cells of the top layer of geotechnical spatial grid based on the real-time seismic load determination module. Accordingly, the PGAs for three earthquake
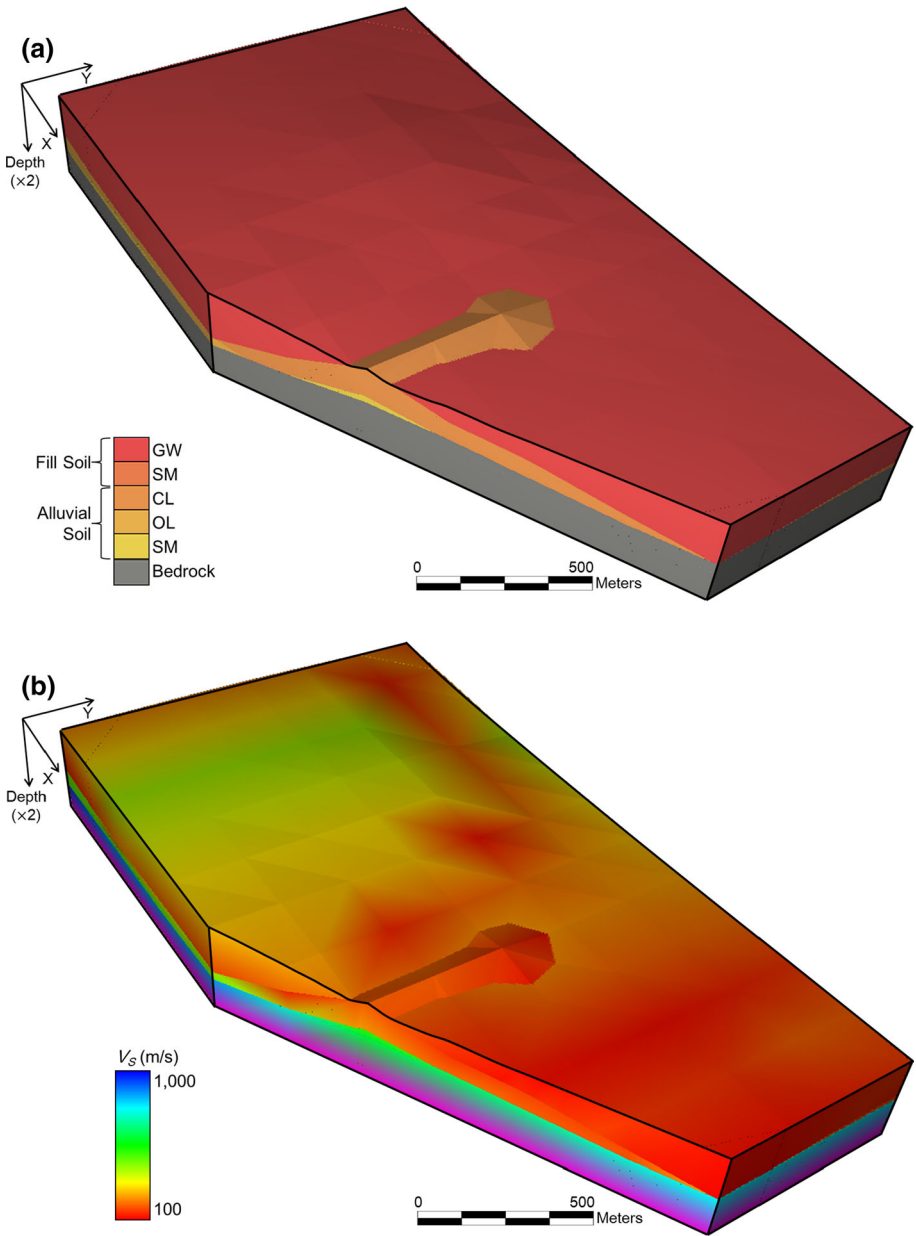
Fig. 14 Three-dimensional projected figures with cross-sectional views of the current ground conditions based on the geotechnical spatial grid in the study area of Incheon Port: **a** geo-layers; **b** shear wave velocity (V_S)

events were calculated at the 2D satellite image (Fig. 15). For the Baengnyeong Island and Taean earthquake events, the actual real-time basis measured and transmitted rock outcrop accelerations were 0.0032 and 0.0064 g (Table 6). And every cells of the geotechnical

spatial grid excepted center zone were corresponded less than 0.01 g. Otherwise, for the 2011 Tohoku earthquake scenario with relatively high rock outcrop acceleration (0.37 g), the 80 % spatial grid of the PGA for the target building was estimated more than 0.40 g.

Near real-time liquefaction spatial grid was automatically estimated using the assigned correlated maximum accelerations of each cell of spatial grid based on the real-time liquefaction hazard estimation module, as shown in Fig. 16. The site-specific liquefaction severity (visualized as grid zones) was determined for the study area according to the LPI criteria by compiling the 3D geotechnical spatial grid assigned with geo-layers and FS$_{liquefaction}$ (Chung et al. 2014). For the Baengnyeong Island and Taean earthquake events, the liquefaction severity for the entire zone of the study area was classified as 'none' (Fig. 15a). After the earthquake events, a simple safety test analysis for the unreinforced concrete structure at the study area (visualized by dotted lines in Fig. 15) indicated that the structure was not affected by liquefaction hazard. In comparison, for the 2011 Tohoku earthquake scenario, the structure occupied most of the cells evaluated as 'extreme' (about 80 % zonation) or 'high' (about 20 % zonation) liquefaction severity class (Fig. 16b). Thus, for the hypothetical earthquake, the liquefaction hazard was extremely severe for the entire study area.

The structure fragilities are estimated automatically based on the real-time earthquake hazard estimation module. For the unreinforced concrete structure in the study area (visualized by the dotted red lines in Fig. 17), the fragility curve (classified as 'slight,' 'moderate,' 'extensive,' and 'complete') of the unreinforced concrete structure is linked with the correlated PGAs based on the geotechnical spatial grid. Consequently, for the two monitored earthquake events, the failure probability in the 'slight' damage level of the
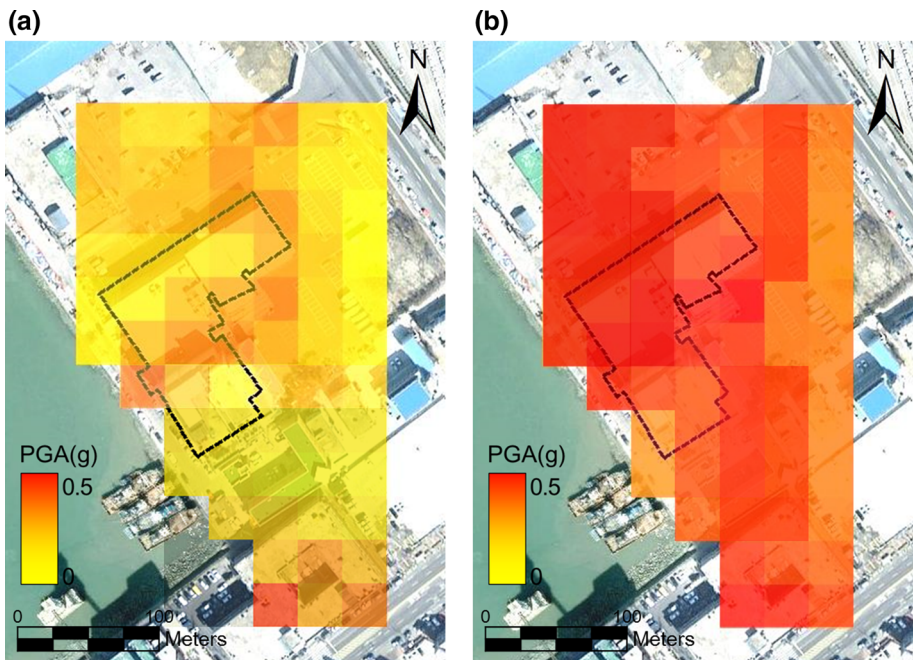

Fig. 15 PGA zonation maps for the target area for three earthquake scenarios: **a** the Baengnyeon Island and Taean earthquake events; **b** the Tohoku earthquake event
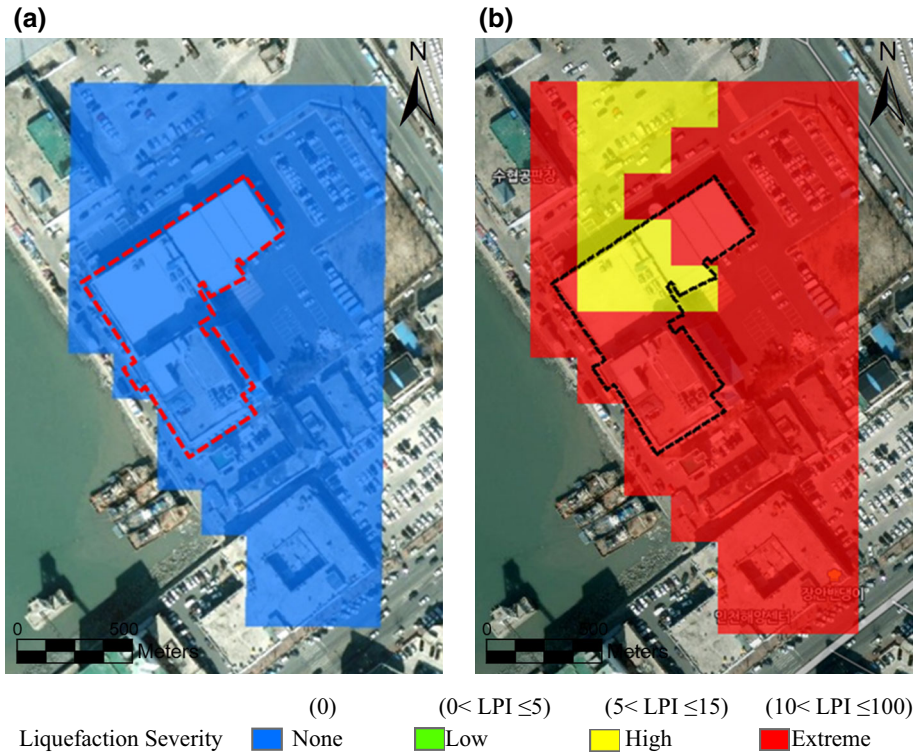
(a)   **(b)**

Liquefaction Severity	(0) None	(0< LPI ≤5) Low	(5< LPI ≤15) High	(10< LPI ≤100) Extreme

Fig. 16 Liquefaction severity zonation maps for the target area for three earthquake scenarios: **a** the Baengnyeon Island and Taean earthquake events; **b** the Tohoku earthquake event

unreinforced concrete structure is calculated by the correlated PGAs based on the geotechnical spatial grid, as shown in Fig. 17. Every cell of the geotechnical spatial grid was evaluated as having a 'safe' damage state ($0 <$ fragility ≤ 50 %). Therefore, the target structure was determined to be safe in terms of seismic fragility. The simple safety test analysis for the target structure indicated that the structure would not fail. For the Tohoku earthquake scenario, the overall study area (which had 40 among 68 cells beneath the target structure) was classified into the 'extensive' damage level. Therefore, the structure was considered to have seismic fragility (having an 80 % damage probability).

6 Conclusions

The developed system, newly built within the frame of GIS, consists of a DB containing all site information and processed data in the system according to the standard formats (DB schema), and system software for performing various functions to manage and utilize the data in the DB. The integrated system consists of the DB and systematic modules. The sub-modules execute various functions for managing and utilizing information in the DB: input of data, geostatistical 3D integrated data based on input data, real-time earthquake hazard data, and output of data.
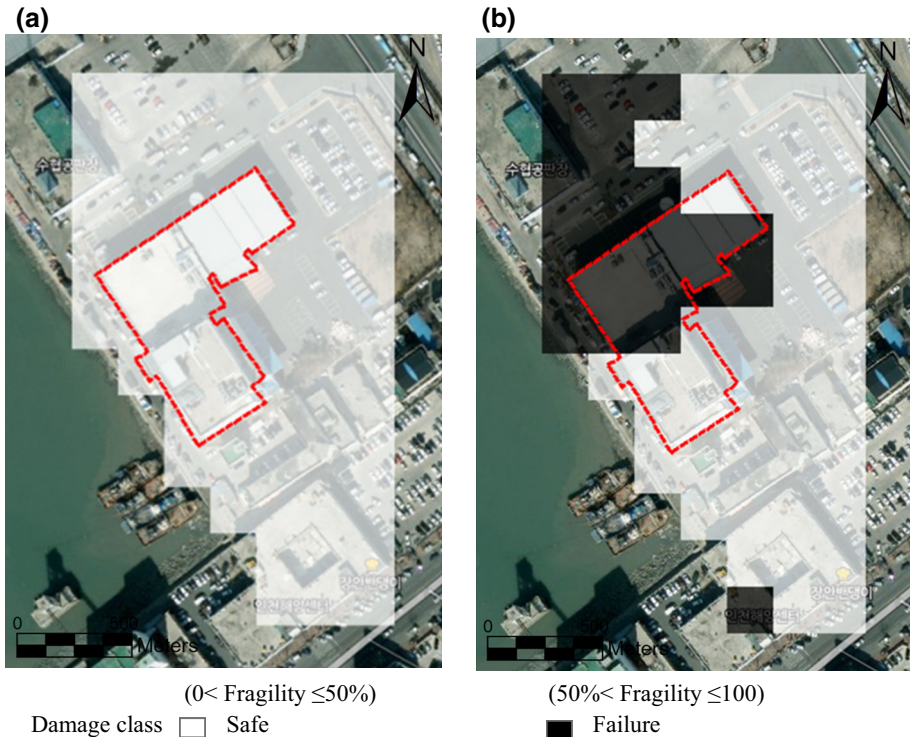
(0< Fragility ≤50%)   (50%< Fragility ≤100)

Damage class   ☐   Safe   ■   Failure

Fig. 17 Structure fragility zonation maps for the target area for three earthquake scenarios: **a** zonation map of the 'slight' damage level for the Baengnyeon Island and Taean earthquake events; **b** zonation map of the 'extensive' damage level for the Tohoku earthquake event

1. DB: The DB stores not only geographic, geotechnical investigative, structural, and seismic monitoring data but also geostatistical 3D integration results and real-time earthquake hazard assessment results.
2. Input function: The input function provides an effective way to store and arrange all collected field data and analysis data according to a standard format based on the GDB.
3. Geostatistical 3D integration for geotechnical spatial grid function: This method has three functional modules with the DB: outlier detection, geostatistical integration, and construction of the geotechnical spatial grid.
4. Real-time earthquake hazard assessment function: The real-time framework has three functional modules with the DB: real-time seismic load determination, real-time liquefaction hazard estimation, and real-time structure fragility evaluation.
5. Output function: The output function displays all attributive information in the DB using tables and graphics according to its characteristics, either on screen or as a document. The earthquake hazard can be visualized and forecasted in real-time with 2D or 3D maps overlain by satellite images.

The DB and these sub-modules of the system software were integrated into a single system, and the developed system provides a familiar and user-friendly working environment with a standard interface. The integrated system is imbedded into the KISS server

for real-time linking of seismic accelerations. We applied it specifically to Incheon Port, Korea, using three earthquake events, based on the GIS platform; 2D and 3D sequential hazard zones were expressed by contours or grid patterns on location maps based on a geotechnical spatial grid to provide more reliable data on liquefaction severity and structure fragility.

As earthquake events actually occur in the target area, the classified spatial zonation of the liquefaction hazard and structure fragility will be concluded in real time. Thus, it is possible to rapidly understand the inherent geotechnical seismic failure at the target site, which is invisible to the naked eye. This systematic application demonstrates that spatial liquefaction hazard and structure fragility can be determined in real time to assist with the decision-making required for earthquake risk management and to develop optimized evacuation paths and restoration plans for port or urban structures. The information acquired by simulation of the developed system could potentially be useful for guiding stabilization projects to prevent secondary disasters and for immediate restoration of transportation lifelines to improve the accessibility of relevant areas.

The developed system was applied to only a few field examples. From the application results, the system was improved by removing bugs and shortcomings. However, there are still some possible improvements that could be made for data availability and compatibility based on DB replication. In addition, other shortcomings may be detected by additional field applications, and these can be improved to develop a more reliable system.

References

American Society for Testing and Materials (1985) Classification of Soils for Engineering Purpose. Annu Book ASTM Stand 4(8):395–408

ATC-13 (1985) Earthquake damage evaluation data for California ATC-13 report. Applied Technology Council, Redwood City, CA

Barnett V, Lewis T (1994) Outliers in statistical data, 3rd edn. Wiley, New York

Borcherdt RD (1994) New developments in estimating site effects on ground motion ATC-35-1, report

Campbell KW, Bozorgnia Y (2003) Updated near-source ground-motion (attenuation) relations for the horizontal and vertical components of peak ground acceleration and acceleration response spectra. Bull Seismol Soc Am 93(1):314–331

Chun SH, Sun CG, Chung CK (2005) Application of geostatistical method for geo-layer information. J Korean Soc Civ Eng 25(2C):103–115

Chun SH, Woo SI, Chung CK, Choi IG (2007a) Development of integrated management system based on GIS on soft ground. J Korean Geotech Soc 23(7):37–46

Chun SH, Woo SI, Chung CK, Choi IG (2007) Integrated construction management system based on GIS for soft ground improvement by preloading. FMGM 2007: seventh international symposium on field measurements in geomechanics, Boston, pp 1–12

Chung CK, Kim HS, Sun CG (2014) Real-time assessment framework of spatial liquefaction hazard in port areas considering site-specific seismic response. Comput Geotech 61:241–253

Cinicioglu SF, Bozbey I, Kelesoglu MK, Oztoprak S, Oztorun NK (2005) An inherent part of urban information systems in earthquake prone areas: Earthquake risk analyses. In: Turkish proceedings of 4th national symposium on infrastructure development, Turkish Society of Civil Engineers, pp 57–68

Cinicioglu SF, Bozbey I, Oztoprak S, Kelesoglu MK (2007) An integrated earthquake damage assessment methodology and its application for two districts in Istanbul, Turkey. Eng Geol 94:145–165

Clayton D, Andre J (1997) GSLIB: geostatistical software library and user's guide. Applied Geostatistics Series

Crowley H, Pihnho R, Bommer JJ (2004) A probabilistic displacement-based vulnerability assessment procedure for earthquake loss estimation. Bull Earthq Eng 2(2):173–219

Drabek TE, Hoetmer GJ (1991) Emergency management: principles and practice for local government. International City Management Association, Washington, DC

ESRI (2006) ArcGIS 9: using ArcGIS desktop. ESRI Press

FEMA (2003) HAZUS-MH Technical Manual. Federal Emergency Management Agency, Washington, DC

Gorvindaraju L, Bhattacharya S (2012) Site-specific earthquake response study for hazard assessment in Kolkata city, India. Nat Hazards 61:943–965

Grubbs FE (1969) Procedures for detecting outlying observations in samples. Technometrics 11:1–21

Hohl P (1998) GIS data conversion: strategies, techniques, and management. OnWord Press, Albany, p 423

International Society for Rock Mechanics (1981) Suggested methods for the quantitative description of discontinuities in rock mass. isrm suggested methods. Pergamon Press

Kim HS (2014) Integrated earthquake hazard assessment system with geotechnical spatial grid information based on GIS. PhD dissertation, Seoul National University

Kim DS, Chung CK, Sun CG, Bang ES (2002) Site assessment and evaluation of spatial earthquake ground motion of Kyeongju. Soil Dyn Earthq Eng 22:371–387

Kim HS, Chun SH, Chung CK (2010) Development of integrated system for management and application of geo-information and underground structures/facilities information based on GIS. 36th Conference of Korean Society of Civil Engineeres, Seoul, Korea, pp 370–373

Kim HS, Cho NG, Chung CK (2012) Real-time LPI-based assessment of the liquefaction potential of the Incheon port in Korea. In: Proceeding of 15th world conference of earthquake engineering, Lisbon, pp 1120–1131

Kim HS, Yoo SH, Jang IS, Chung CK (2012b) Real-time seismic damage estimation for harbor site considering ground motion amplification characteristics. J Earthq Eng 28(5):55–65

King SA, Kiremidjian AS (1994) Regional seismic hazard and risk analysis through geographic information systems. Blume Center Reports, report no. 111. Stanford University, Palo Alto, p 185

Koltermann CE, Gorelick S (1996) Heterogeneity in sedimentary deposits: a review of structure-imitating, processimitating, and descriptive approaches. Water Resour Res 32(9):2617–2658

Korte GB (1997) The GIS book: understanding the value and implementation of geographic information systems. OnWord Press, Albany, p 440

Kupfersberger H, Deutsch CV (1999) Methodology for integrating analog geologic data in 3D variogram modelling. AAPG Bulletin 83(8):1262–1278

Lee J, Wong DWS (2001) Statistical analysis with ArcView GIS. Wiley, Canada

Marble DF, Pequet DJ (1983) Geographic information system and remote sensing, in manual of remote sensing. American Society of Photogrammetry, Falls Church

Mouroux P, Le BB (2006) Risk-UE project: an advanced approach to earthquake risk scenarios with application to different European towns. In: Oliveira CS, Roca A, Goula X (eds) Assessing and managing earthquake risk. Springer, Dordrecht

Pal I, Nath SK, Shukla K, Pal DK, Raj A, Thingbaijam KKS, Bansal BK (2008) Earthquake hazard zonation of Sikkim Himalaya using a GIS platform. Nat Hazards 45(3):333–377

Papadimitriou AG, Antoniou AA, Bouckovalas GD, Marinos PG (2008) Methodology for automated GIS-aided seismic microzonation studies. Comput Geotech 35:505–523

RADIUS (1999) Risk assessment tools for diagnosis of urban areas against seismic disasters. United Nations initiative towards Earthquake Safe cities. http://www.geohaz.org/radius/

Schneider PJ, Schauer BA (2006) HAZUS—its development and its future. Nat Hazards Rev 7:40–44

Sun CG (2004) Geotechnical information system and site amplification characteristics for earthquake ground motions at inland of the Korean Peninsula. PhD dissertation, Seoul National University, Seoul, Korea

Sun CG, Chun SH, Ha TG, Chung CK, Kim DS (2008) Development and application of GIS-based tool for earthquake-induced hazard prediction. Comput Geotech 35(3):436–449

Sun CG, Shin JS, Chi HC (2009) Regional estimation of site-specific seismic response by spatial zoning on site period at Daegu in Korea. In: Proceedings of the 3rd IASME/WSEAS international conference on geology and seismology (GES'09), Cambridge, pp 85–90

Sun CG, Kim BH, Park KH, Chung CK (2015) Geotechnical comparison of weathering degree and shear wave velocity in the decomposed granite layer in Hongseong, South Korea. Environ Earth Sci 74(9):6901–6917

Thomas JB, Paul WB (2013) Seismic hazard across Bulgaria and neighbouring areas: regional and site-specific maximum credible magnitudes and earthquake perceptibility. Nat Hazards 68:271–319

Toprak S, Holzer TL (2003) Liquefaction potential index: field assessment. J Geotech Geoenviron Eng ASCE 129:315–322

Vahidnia MH, Alesheikh AA, Alimohammadi A, Hosseinali FA (2010) GIS-based neuro-fuzzy procedure for integrating knowledge and data in landslide susceptibility mapping. Comput Geosci 36:1101–1114

Wair BR, DeJong JT, Shantz T (2012) Guidelines for estimation of shear wave velocity profiles. Pacific Earthquake Engineering Research Center, PEER report 8

Weissmann GS, Carle SF, Fogg GE (1999) Threedimensional hydrofacies modeling based on soil surveys and transition probability geostatistics. Water Resour Res 35(6):1761–1770

Xu L, Liu G (2009) The study of a method of regional environmental risk assessment. J Environ Manag 90(3):290–296

Yeh CH, Loh CH, Tsai KC (2006) Overview of Taiwan earthquake loss estimation system. Nat Hazards 37:23–27

Youd TL, Perkins DM (1978) Mapping liquefaction-induced ground failure potential. Journal of the Geotechnical Engineering 104:433–446